

Platform for Advanced Scientific Computing Conference  
PASC19, June 12, 2019, ETH-Zürich, Mini Symposion M11:  
Multidimensional Stellar Evolution: Bridging the Modelling and Computational Challenges

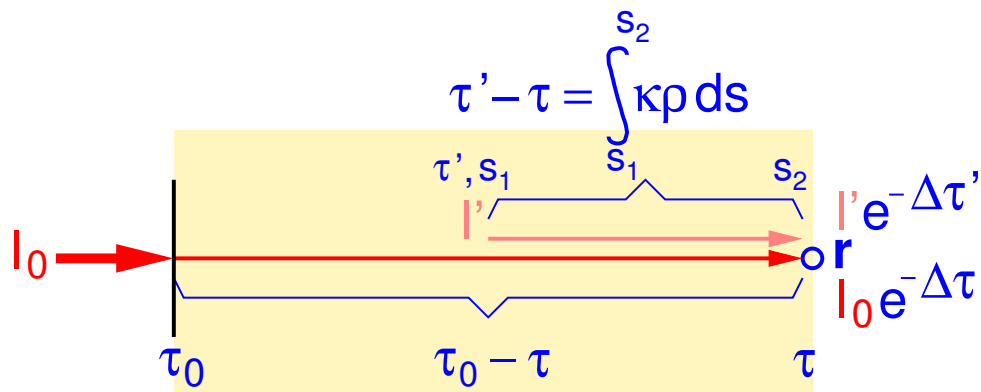
## **Aspects of multi-dimensional radiation transfer in stellar atmospheres**

---

*Oskar Steiner*

Istituto Ricerche Solari Locarno (IRSOL), Locarno and  
Leibniz-Institut für Sonnenphysik (KIS), Freiburg i.Br.

# 1. Introduction



$\kappa_\nu$ : opacity per unit mass [ $\text{cm}^2 \text{g}^{-1}$ ]  
 $\tau$ : optical distance to  $\mathbf{r}$

*Formal solution* of the  
radiative transfer equation

$$I(\mathbf{r}, \mathbf{n}) = I_0 e^{-(\tau_0 - \tau)} + \int_{\tau}^{\tau_0} S(\tau') e^{-(\tau' - \tau)} d\tau'$$

For short:  $I(\mathbf{r}, \mathbf{n}) = \Lambda S$  (Lambda operator)

The *radiative transfer equation*

$$\frac{dI_\nu}{d\tau_\nu} = I_\nu - S_\nu$$

$$\frac{dI_\nu}{ds} = -\kappa_\nu \rho (I_\nu - S_\nu)$$

$I = I(\mathbf{r}, \hat{\mathbf{n}}, \nu, t)$  has dimension [ erg  $\text{cm}^{-2} \text{s}^{-1} \text{hz}^{-1} \text{sr}^{-1}$  ]

## 1. Introduction (cont.)

$$\text{Radiative flux} \quad \mathbf{F}_{\text{rad}} = \int_{4\pi} \int_0^\infty I(\mathbf{r}, \hat{\mathbf{n}}, \nu) \hat{\mathbf{n}} \, d\nu \, d\omega \quad [\text{erg cm}^{-2} \text{ s}^{-1}]$$

Using the radiative transfer equation we obtain for the divergence of the radiative flux:

$$\begin{aligned} \nabla \cdot \mathbf{F}_{\text{rad}} &= \int_{4\pi} \int_0^\infty (\hat{\mathbf{n}} \cdot \nabla) I(\mathbf{r}, \hat{\mathbf{n}}, \nu) \, d\nu \, d\omega \\ &= \int_{4\pi} \int_0^\infty (\kappa(\mathbf{r}, \nu) \rho(\mathbf{r}) S(\mathbf{r}, \nu) - \kappa(\mathbf{r}, \nu) \rho(\mathbf{r}) I(\mathbf{r}, \hat{\mathbf{n}}, \nu)) \, d\nu \, d\omega \\ &= 4\pi \int_0^\infty \kappa(\mathbf{r}, \nu) \rho(\mathbf{r}) (S(\mathbf{r}, \nu) - J(\mathbf{r}, \nu)) \, d\nu = -q_{\text{rad}} \end{aligned}$$

With  $J(\mathbf{r}, \nu) = \frac{1}{4\pi} \int_{4\pi} I(\mathbf{r}, \hat{\mathbf{n}}, \nu) \, d\omega$  being the *mean intensity*.

## 2. Radiation transfer for stellar atmospheric simulations

---

The equations of ideal magnetohydrodynamics in *conservation law form*:

$$\boxed{\frac{\partial \mathbf{U}}{\partial t} + \nabla \cdot \mathcal{F} = \mathbf{S},}$$

where the *vector of conserved variables*  $\mathbf{U}$ , the *source term*  $\mathbf{S}$  due to gravity and radiation, and the *flux tensor*  $\mathcal{F}$  are

$$\mathbf{U} = (\rho, \rho\mathbf{v}, \mathbf{B}, E) , \quad \mathbf{S} = (0, \rho\mathbf{g}, 0, \rho\mathbf{g} \cdot \mathbf{v} + q_{\text{rad}}) ,$$

$$\mathcal{F} = \begin{pmatrix} \rho\mathbf{v} \\ \rho\mathbf{v}\mathbf{v} + \left(p + \frac{\mathbf{B} \cdot \mathbf{B}}{8\pi}\right) \mathbf{I} - \frac{\mathbf{B}\mathbf{B}}{4\pi} \\ \mathbf{v}\mathbf{B} - \mathbf{B}\mathbf{v} \\ \left(E + p + \frac{\mathbf{B} \cdot \mathbf{B}}{8\pi}\right) \mathbf{v} - \frac{1}{4\pi} (\mathbf{v} \cdot \mathbf{B}) \mathbf{B} \end{pmatrix} .$$

## 2. Radiation transfer for stellar atmospheric simulations (cont.)

The total energy density  $E$  is given by

$$E = \rho\epsilon + \rho\frac{\mathbf{v} \cdot \mathbf{v}}{2} + \frac{\mathbf{B} \cdot \mathbf{B}}{8\pi},$$

where  $\rho$ : mass density;  $\mathbf{v}$ : velocity;  $P$ : gas pressure;  $\mathbf{B}$ : magnetic field;  $\mathbf{g}$ : gravitational acceleration;  $e_{\text{int}}$ : thermal energy per unit mass;  $\mathbf{F}_{\text{rad}}$ : radiative flux;  $t$ : time.

Alternatively, we can define

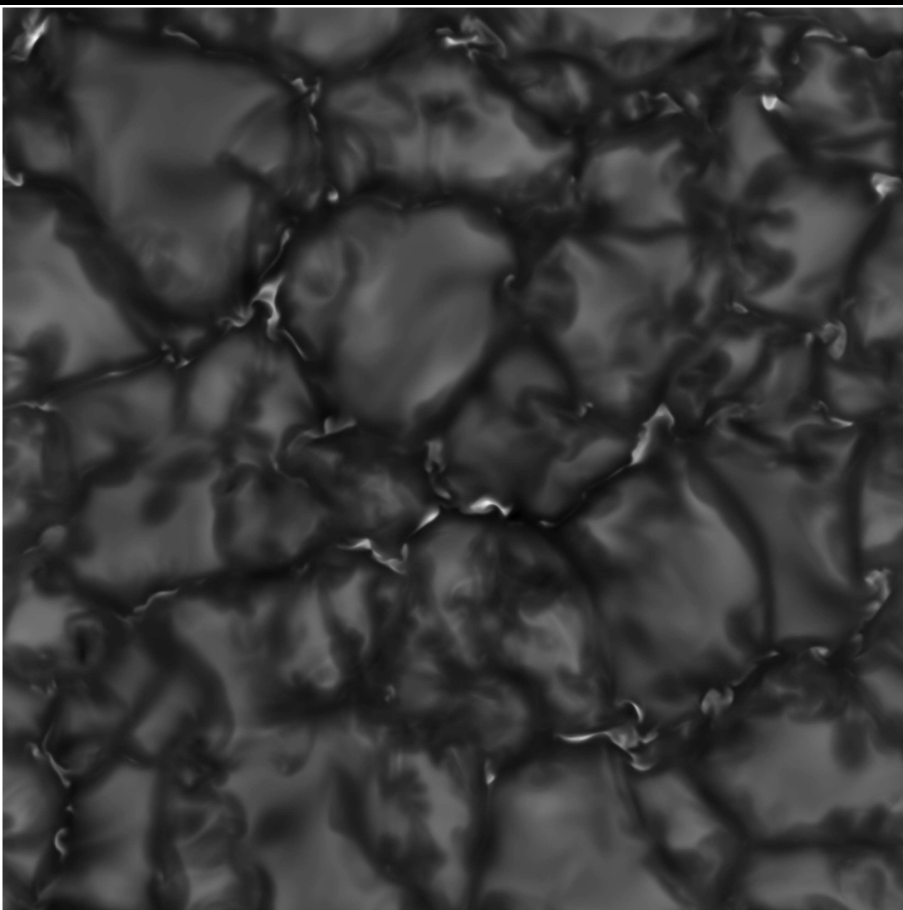
$$E = \rho e_{\text{int}} + e_{\text{kin}} + e_{\text{mag}} + e_{\text{pot}} = \rho e_{\text{int}} + \rho\frac{\mathbf{v} \cdot \mathbf{v}}{2} + \frac{\mathbf{B} \cdot \mathbf{B}}{2} + \rho\Phi$$

in which case the energy equation can be written in strict conservative form:

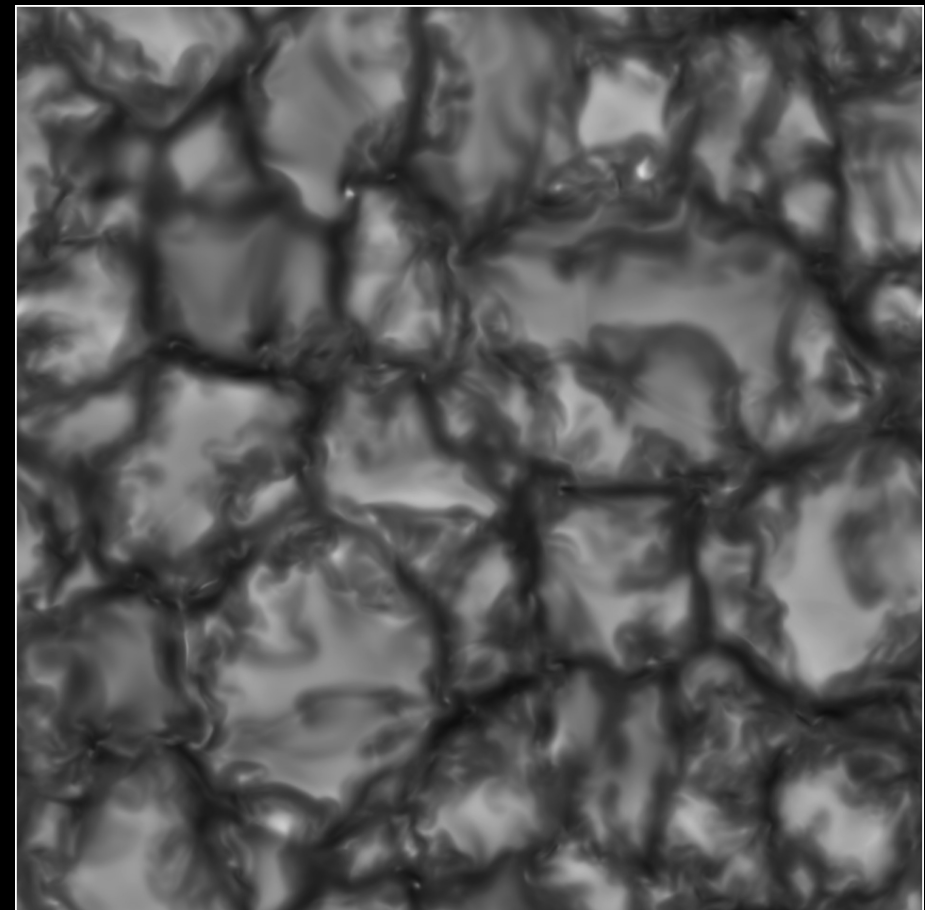
$$\frac{\partial \rho e_{\text{tot}}}{\partial t} + \nabla \cdot \left( \left( \rho e_{\text{tot}} + P + \frac{\mathbf{B} \cdot \mathbf{B}}{2} \right) \mathbf{v} - (\mathbf{v} \cdot \mathbf{B}) \mathbf{B} + \mathbf{F}_{\text{rad}} \right) = 0$$

## 2. Radiation transfer for stellar atmospheric simulations (cont.)

Bolometric intensity maps



With magnetic fields:  
Magnetohydrodynamic simulation.



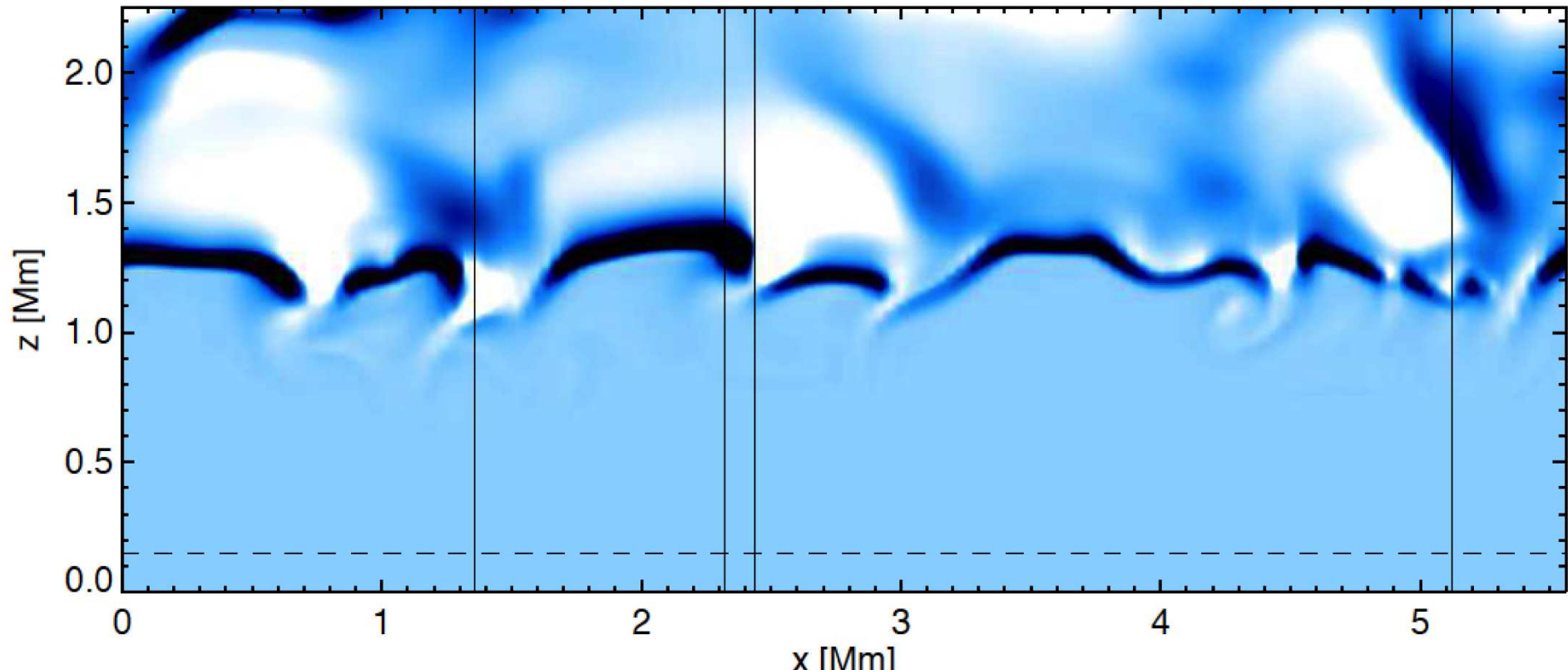
Without magnetic fields:  
Hydrodynamic simulation

Courtesy,  
*F. Calvo.*

Computations: *Centro Svizzero di Calcolo Scientifico*

## 2. Radiation transfer for stellar atmospheric simulations (cont.)

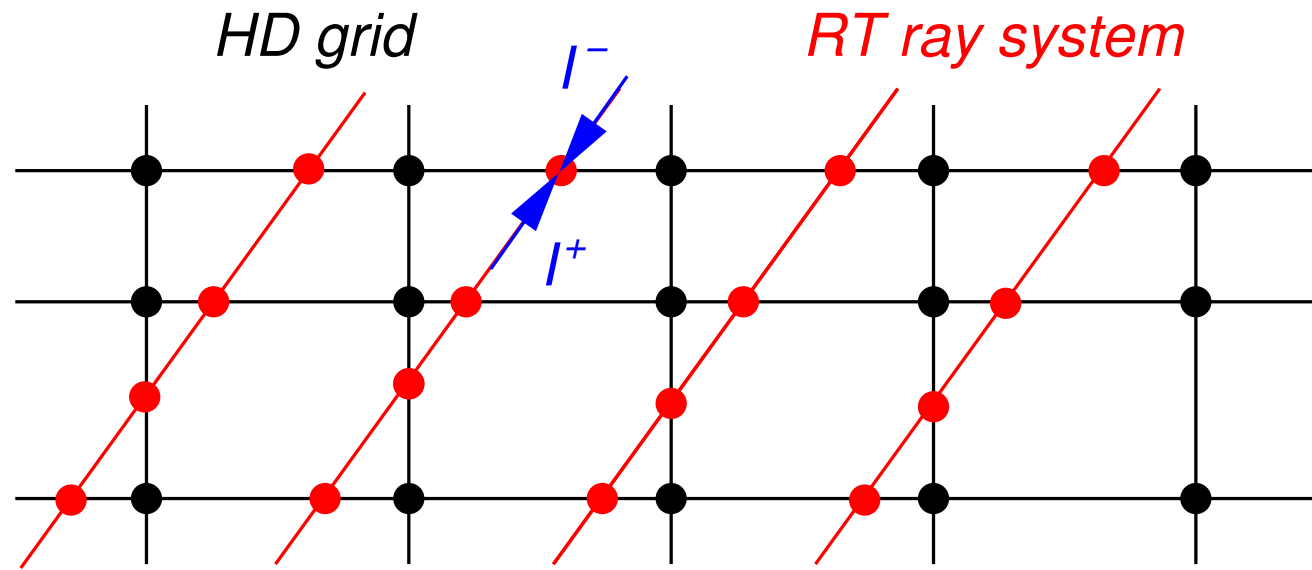
$q_{\text{rad}}$  (*per unit mass*) in a vertical section through a 3D solar model.  $z = 1.3 \text{ Mm}$  corresponds to  $\langle \tau_{500} \rangle = 1$ . *Dark/bright* shades indicate *radiative cooling/heating*.



From *Steffen (2017)*.

## 2. Radiation transfer for stellar atmospheric simulations (cont.)

### Integration on long characteristics



HD grid:  $\rho, e \xrightarrow{\text{EOS}} p, T \rightarrow$  source function  $S$ , opacity  $\rho\kappa$

$\rightarrow$  interpolation  $\rightarrow$  RT Rays system:  $S, \rho\kappa$

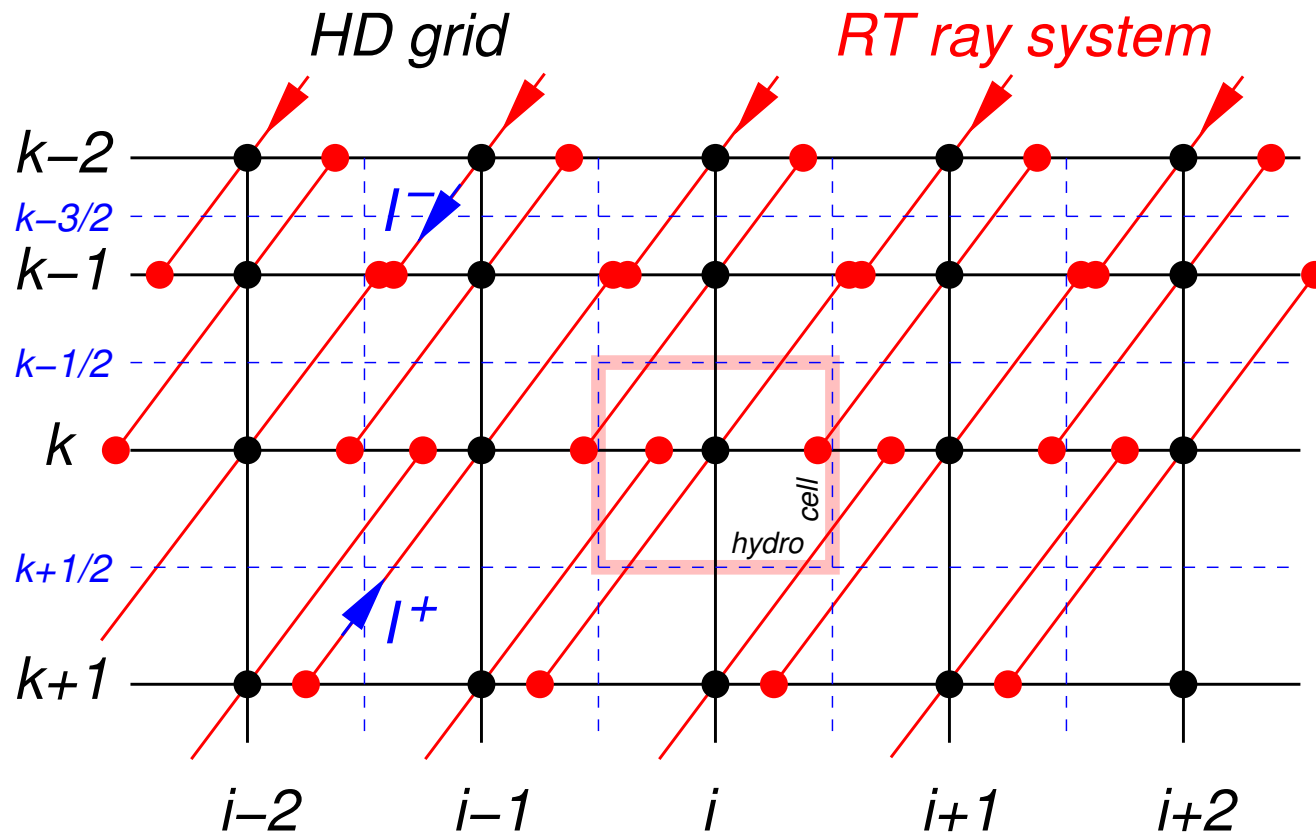
$\rightarrow$  solve RT for  $y_\nu = (1/2)(I_\nu^+ + I_\nu^-) - S_\nu$  (Feautrier scheme)

RT Ray system:  $\rho\kappa y_\nu = q_{\text{rad}}^{\theta, \phi} \rightarrow$  flux conservative back-interpolation

$\rightarrow$  HD grid:  $q_{\text{rad}}^{\theta, \phi} \rightarrow \sum_{\theta, \phi} q_{\text{rad}}^{\theta, \phi} = q_{\text{rad}}$

## 2. Radiation transfer for stellar atmospheric simulations (cont.)

### Integration on short characteristics



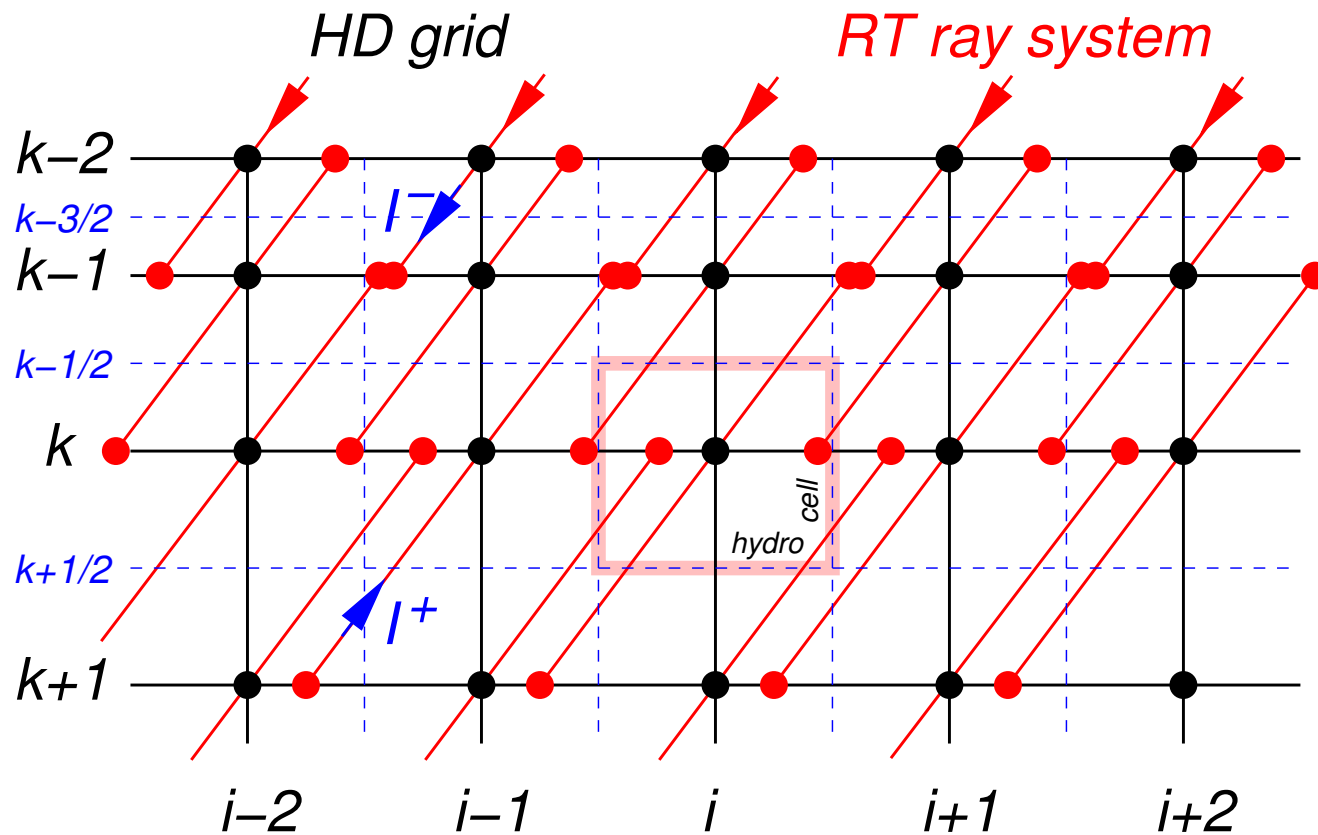
RT Rays system: start at top compute  $I^-$ , start at bottom compute  $I^+$

$$\rightarrow q_{\text{rad}}(\theta, \phi) = q_{\text{rad}}^-(\theta, \phi) + q_{\text{rad}}^+(\theta, \phi)$$

important: flux conservative interpolation of intensities

## 2. Radiation transfer for stellar atmospheric simulations (cont.)

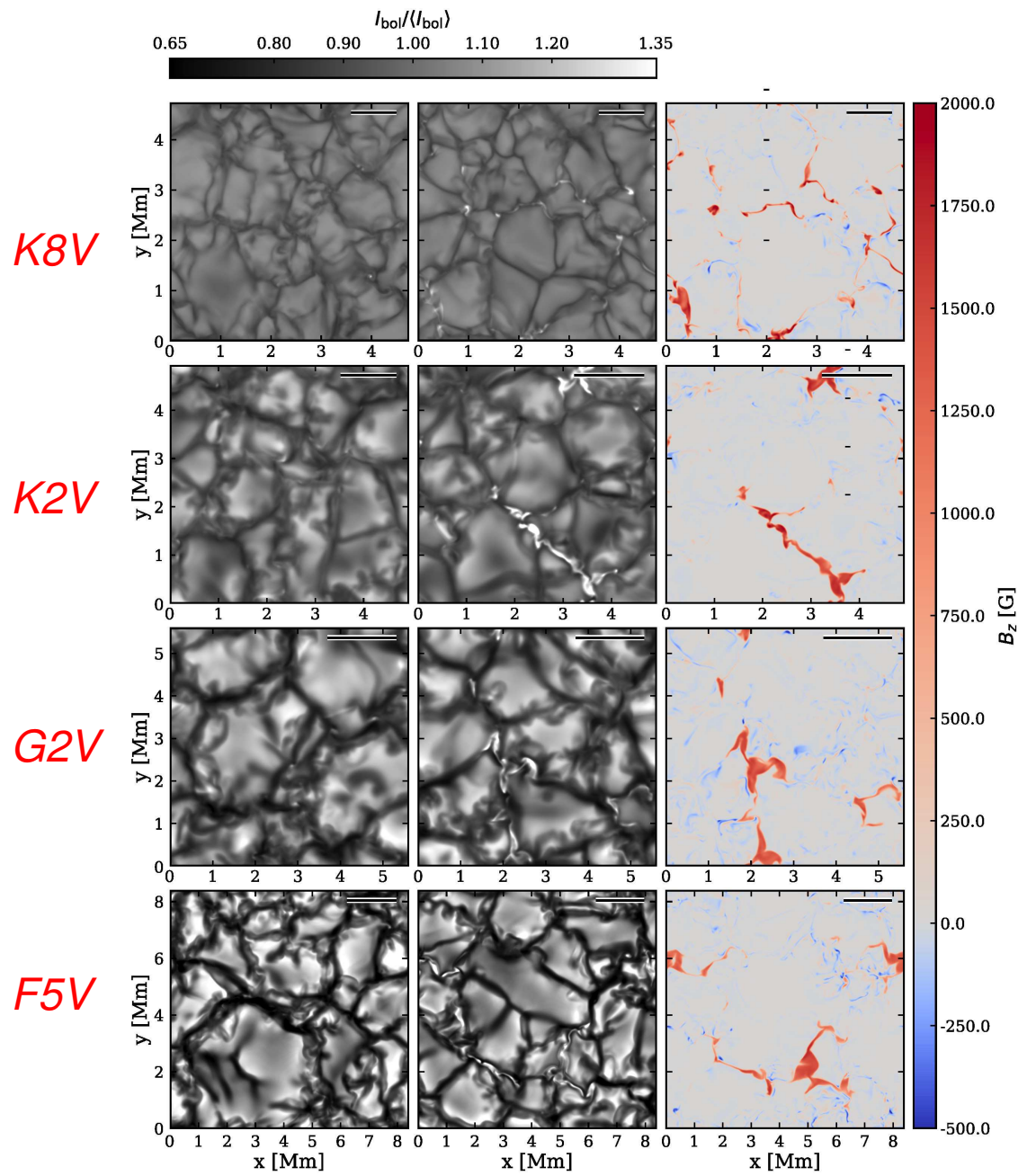
### Conservation of radiative flux



$$\int_x \int_y F_{\text{rad}}^{k-\frac{1}{2}} dx dy - \int_x \int_y F_{\text{rad}}^{k+\frac{1}{2}} dx dy = \int_x \int_y \int_{z_{k+1/2}}^{z_{k-1/2}} -q_{\text{rad}}(x, y, z) dx dy dz$$

Adapted from *Steffen (2017)*.

## 2. Radiation transfer for stellar atmospheric simulations (cont.)



- “*Box in a star*” simulations of the surface layers of four spectral types;
- Each simulation is *run twice*: with and without magnetic fields;
- Initial vertical homogeneous field of **50 G** and **100 G**;
- Multi-group *radiation transfer* using 5 opacity bins;
- From *Salhab et al. (2018, A&A 614, A78)*.

### 3. Multi-group radiation transfer

*Nordlund, 1982; Ludwig, 1992*

---

$$q_{\text{rad}} = -\nabla \cdot \mathbf{F}_{\text{rad}} = 4\pi\rho \int \kappa_\lambda (J_\lambda - B_\lambda) d\lambda,$$

$$\begin{aligned} \int \kappa_\lambda (J_\lambda - B_\lambda) d\lambda &= \sum_j \kappa_{\lambda_j} (J_{\lambda_j} - B_{\lambda_j}) w_{\lambda_j} \\ &= \sum_i \sum_{j(i)} \kappa_{\lambda_j} (J_{\lambda_j} - B_{\lambda_j}) w_{\lambda_j} \\ &= \sum_i \sum_{j(i)} \kappa_{\lambda_j} (\Lambda_{\lambda_j} (B_{\lambda_j}) - B_{\lambda_j}) w_{\lambda_j} \\ &\approx \sum_i \kappa_i (\Lambda_i - 1) \left( \sum_{j(i)} B_{\lambda_j} w_{\lambda_j} \right) \\ &\doteq \sum_i \kappa_i (\Lambda_i - 1) (B_i w_i) \doteq \sum_i \kappa_i (J_i - B_i) w_i \end{aligned}$$

### 3. Multi-group radiation transfer (cont.)

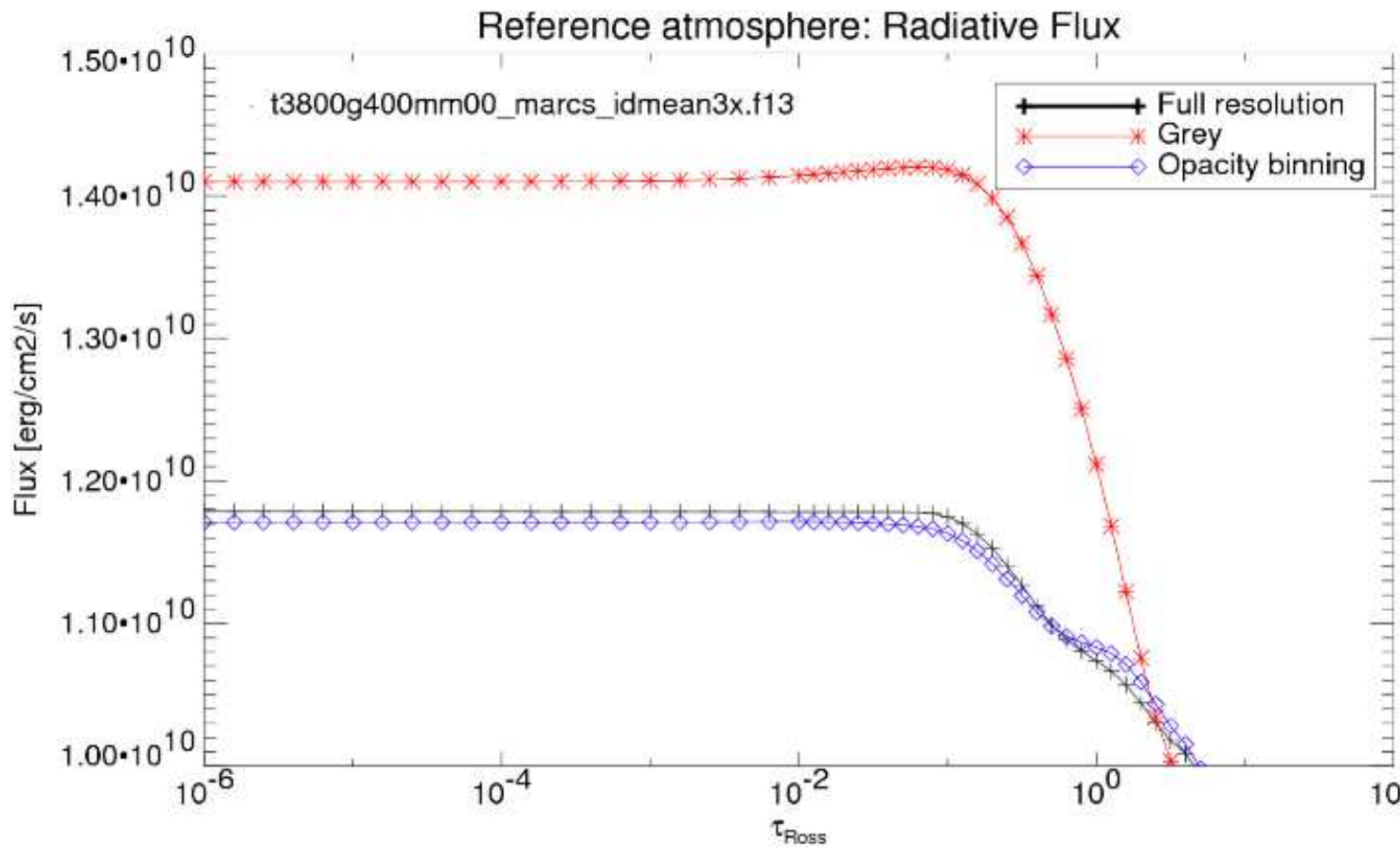
Strategy for opacity binning:

- concentrate on radiative transfer in vertical direction,
- group together frequencies with as similar a  $\tau_\nu(s)$ -relationship as possible, so that  $\Lambda_{\lambda_j(i)}$  is very similar  $\forall j$  of a given bin  $i$ ,
- choose clever averaging procedure for  $\kappa_\nu$ , (Rosseland averages for  $\tau_i > 1$ , Planck averages for  $\tau_i < 1$ ).

See also *Nordlund, Å: 1982, A&A 107,1; Ludwig, H.-G.: 1992, thesis Univ. Kiel; Vögler et al.: 2001, A&A 421, 741; Hayek et al.: 2010, A&A 517,A49.*

### 3. Multi-group radiation transfer (cont.)

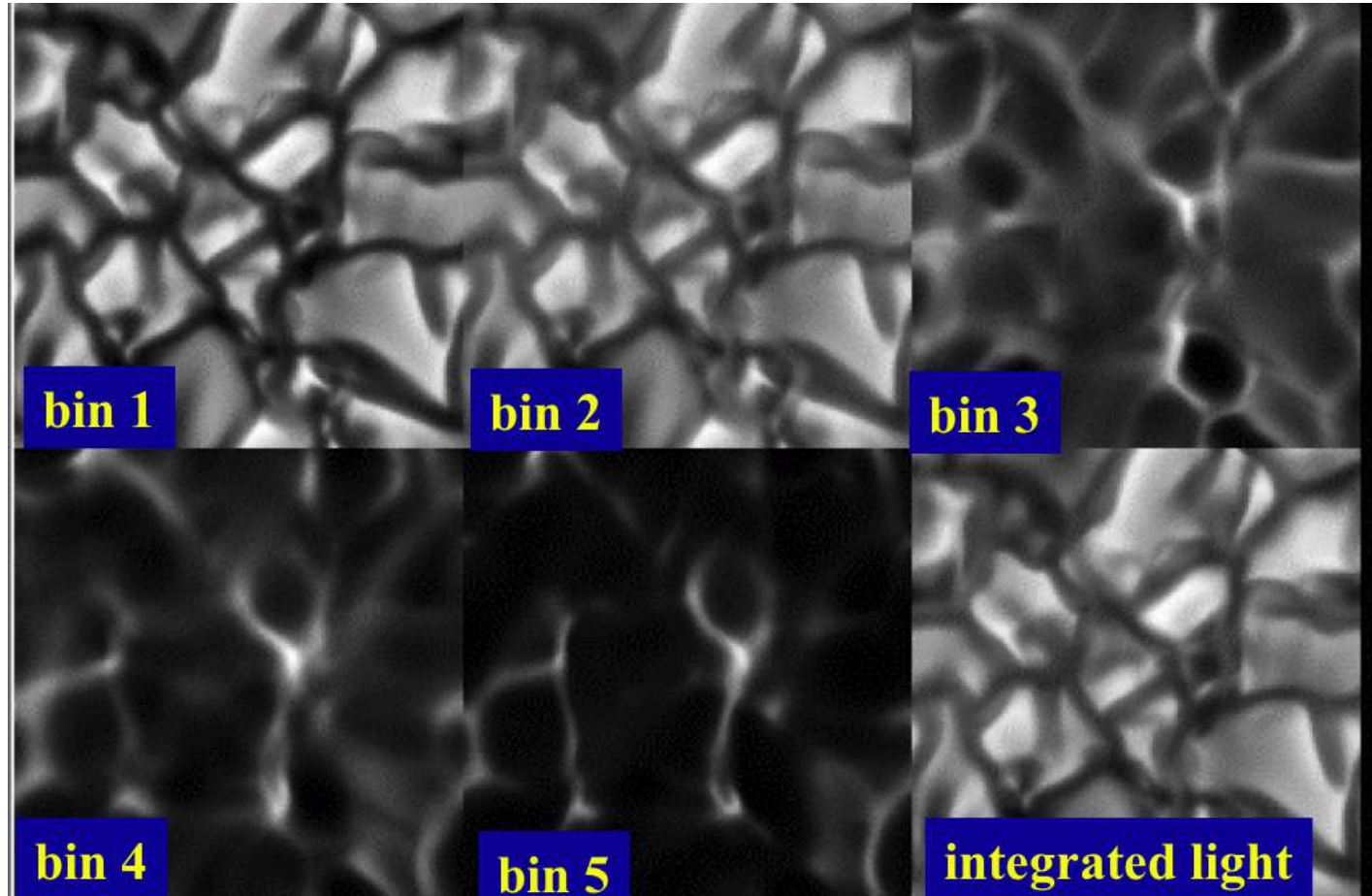
#### Testing the OBM. Integrated radiative flux



Courtesy, M. Steffen.

### 3. Multi-group radiation transfer (cont.)

Intensity maps for different opacity bins



Courtesy, M. Steffen.

Notice that bin 3 to 5 show “inverse granulation” as their opacities represent medium to strong line cores.

## 4. Spectral line analysis

---

The purpose of radiative transfer performed in the course of the simulation is to take the exchange of energy between matter and radiation properly into account.

For the *detailed study of spectral lines*, radiation transfer is carried out in a *post-processing step*, after the simulation.

For this, we consider a “frozen” time instant of the simulation and assume *statistical equilibrium*. Then, the population of the  $i$ -th level of the atom that produces the spectral line is governed by

$$\underbrace{n_i \sum_{j \neq i}^N P_{ij}}_{\text{transitions from } i \text{ to other levels}} = \underbrace{\sum_{j \neq i}^N n_j P_{ji}}_{\text{transitions from others to level } i} .$$

$n_i$  is the number density of atoms with electronic occupation of level  $i$  and  $P_{ij}$  is the probability per unit time for a transition from level  $i$  to level  $j$  with dimension  $[s^{-1}]$ .

$N$  is the number of bound levels (we discard transitions to and from the continuum).

## 4. Spectral line analysis (cont.)

As an additional (closure) equation we have the *particle number conservation*:

where  $\epsilon$  is the abundance of the considered chemical element relative to hydrogen  $n_{\text{H}}$ .

For the  $N$ -level atom we have then for each spatial grid point the following *linear system for the occupation numbers*:

$$\mathcal{W}\mathbf{n} = \mathbf{f}$$

$$\mathcal{W} = \begin{pmatrix} 1 & 1 & \dots & 1 & 1 \\ P_{1,2} & -\sum & \dots & P_{N-1,2} & P_{N,2} \\ \vdots & \vdots & \ddots & \vdots & \vdots \\ P_{1,N} & P_{2,N} & \dots & \dots & -\sum \end{pmatrix}; \quad \mathbf{n} = \begin{pmatrix} n_1 \\ n_2 \\ \vdots \\ n_N \end{pmatrix}; \quad \mathbf{f} = \begin{pmatrix} \epsilon n_{\text{H}} \\ 0 \\ \vdots \\ 0 \end{pmatrix},$$

where  $\sum = \sum_{j=1, j \neq i}^N P_{ij}$  is the total rate of outgoing transitions from level  $i$  to any other level  $j$ .

## 4. Spectral line analysis (cont.)

$P_{ij} = C_{ij} + R_{ij}$  consists of the *collisional rate*  $C_{ij}$  and the *radiative rate*  $R_{ij}$ .

$$R_{ij} = \begin{cases} A_{ij} + B_{ij} \bar{J}_{ij} & \text{if } i > j \quad \text{for spontaneous and induced emission,} \\ B_{ji} \bar{J}_{ji} & \text{if } i < j \quad \text{for absorption,} \end{cases}$$

where  $A_{ij}$ ,  $B_{ij}$ , and  $B_{ji}$  are the Einstein coefficients.  $\bar{J}$  is the mean intensity

$$\bar{J}_{ij} = \bar{J}_{ji} = \frac{1}{4\pi} \iint I_\nu \phi(\nu) d\nu d\Omega .$$

## 4. Spectral line analysis (cont.)

The net gain of photonic energy through transitions between  $i$  and  $j$  is then given by

$$h\nu[n_i(A_{ij} + B_{ij}\bar{J}_{ij}) - n_jB_{ji}\bar{J}_{ij}] = h\nu n_i A_{ij} + h\nu(n_i B_{ij} - n_j B_{ji})\bar{J}_{ij}$$

which corresponds to the integral right hand side of the radiative transport equation

$$\frac{dI_\nu}{ds} = -\kappa\rho(I_\nu - S_\nu),$$

from which it follows the *opacity and source* due to the transition between levels  $i$  and  $j$ ,

$$\kappa_{ij} = \frac{h\nu}{4\pi\rho}(n_j B_{ji}\phi(\nu) - n_i B_{ij}\psi(\nu)); \quad S_{ij} = \frac{n_i A_{ij}\chi(\nu)}{n_j B_{ji}\phi(\nu) - n_i B_{ij}\psi(\nu)}.$$

Often we assume  $\chi = \psi = \phi$  (complete redistribution) but for the wings of some important spectral lines formed in the solar chromosphere this is a bad approximation (partial redistribution).

## 4. Spectral line analysis (cont.)

One row of the statistical equilibrium equations reads in expanded form

$$\sum_{j < i} [n_i A_{ij} - (n_j B_{ji} - n_i B_{ij}) \bar{J}_{ij}] - \sum_{j > i} [n_j A_{ji} - (n_i B_{ij} - n_j B_{ji}) \bar{J}_{ij}] + \sum_j (n_i C_{ij} - n_j C_{ji}) = 0.$$

It is still a linear equation in the level population vector  $\mathbf{n}$ , discarding the dependency of  $\bar{J}_{ij}$  on the level populations.

$$\bar{J}_{ij} = \frac{1}{4\pi} \iint I_\nu \phi(\nu) d\nu d\Omega, \quad \text{where} \quad \frac{dI_{ij}}{ds} = -\kappa_{ij} \rho (I_{ij} - S_{ij}), \quad \text{and}$$

$$S_{ij} = \frac{n_i A_{ij}}{n_j B_{ji} - n_i B_{ij}},$$

$$\kappa_{ij} = \frac{h\nu}{4\pi\rho} (n_j B_{ji} - n_i B_{ij}).$$

For short:

$$\boxed{\bar{J}_{ij} = \Lambda_{ij} \mathbf{S}_{ij}}$$

## 4. Spectral line analysis (cont.)

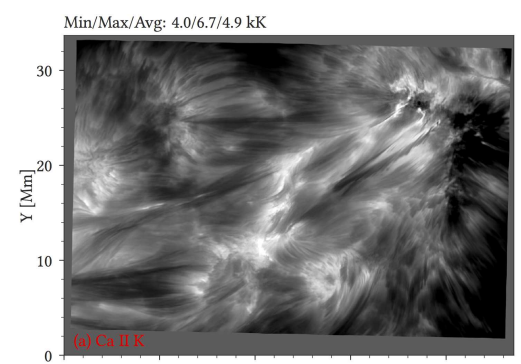
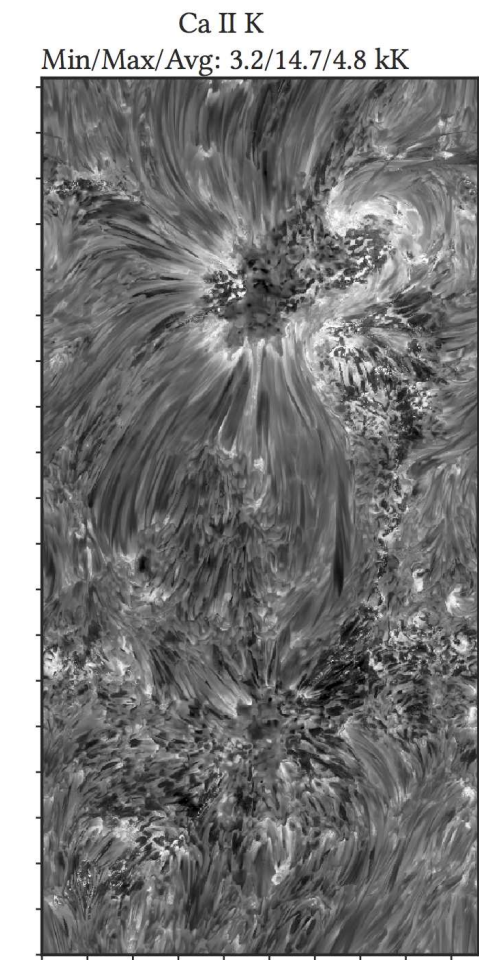
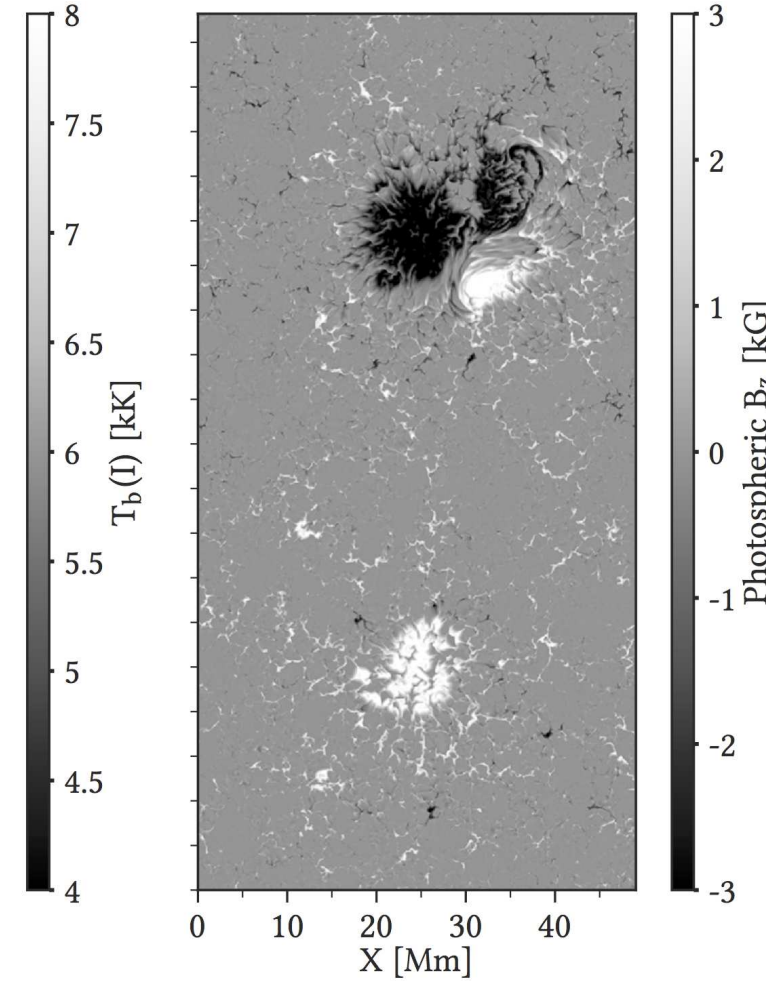
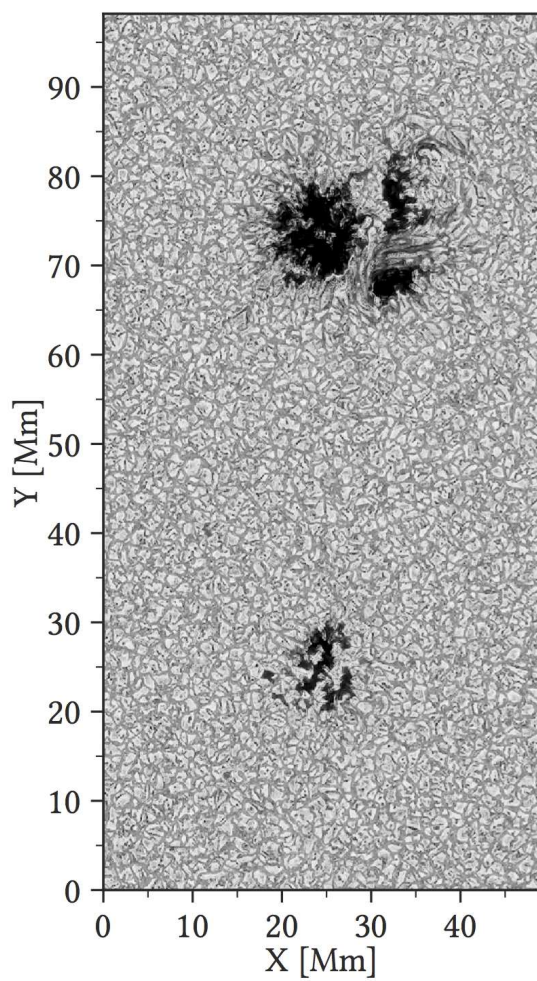
Remedy operator perturbation:

$$\begin{aligned}\bar{J}_{ij} &= \Lambda_{ij}^* \mathbf{S}_{ij} + (\Lambda_{ij} - \Lambda_{ij}^*) \mathbf{S}_{ij}^{\text{old}} \\ \Lambda_{ij} &= \Lambda_{ij}^* + (\Lambda_{ij} - \Lambda_{ij}^*) \\ &= \Lambda_{ij}^* \mathbf{S}_{ij} + \mathbf{J}_{ij}^{\text{old}} - \Lambda_{ij}^* \mathbf{S}_{ij}^{\text{old}} \\ &= \Lambda_{ij}^* \mathbf{S}_{ij} + \mathbf{J}_{ij}^{\text{res}}\end{aligned}$$

$$\begin{aligned}&\sum_{j < i} [n_i(1 - \Lambda_{ij}^*) A_{ij} - (n_j B_{ji} - n_i B_{ij}) \bar{J}_{ij}^{\text{res}}] \\ &- \sum_{j > i} [n_j(1 - \Lambda_{ij}^*) A_{ji} - (n_i B_{ij} - n_j B_{ji}) \bar{J}_{ij}^{\text{res}}] \\ &+ \sum_j (n_i C_{ij} - n_j C_{ji}) = 0.\end{aligned}$$

Jacobi-like iteration, accelerated  $\Lambda$ -iteration

## 4. Spectral line analysis (cont.)



*Ca II K line core image* (top row rightmost panel) of a simulated active region (top row) in comparison to Ca II K image of an observed active region (bottom panel).

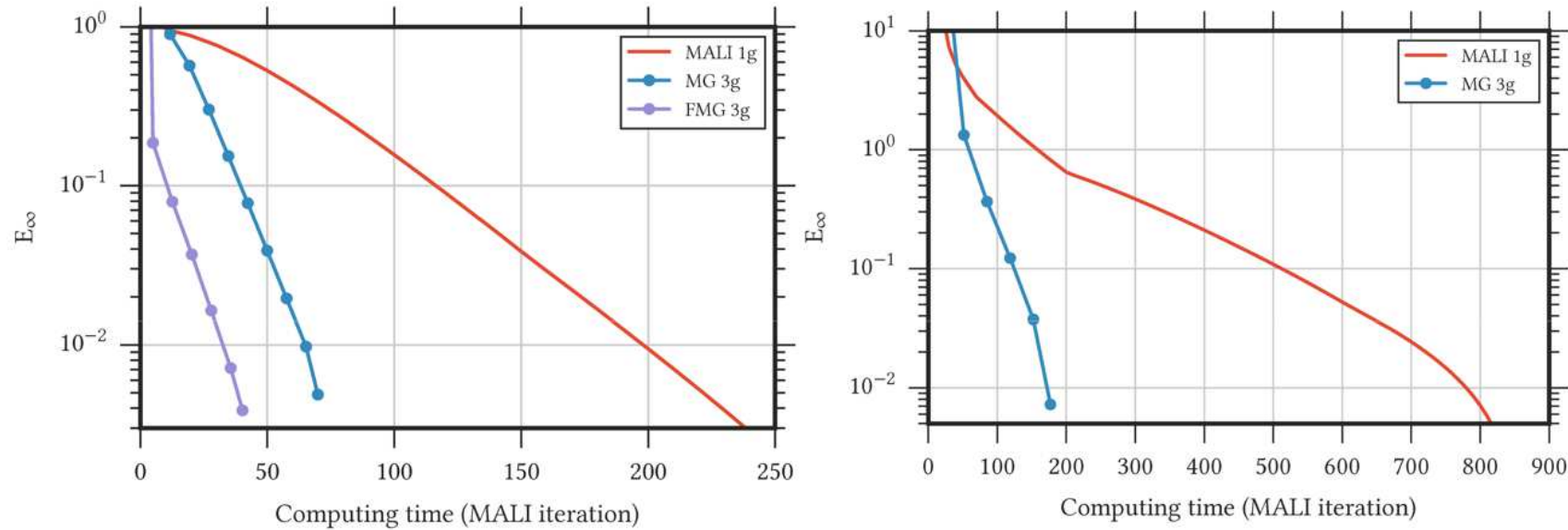
From *Bjørgen et al., 2019*.

## 4. Spectral line analysis (cont.)

### Multigrid radiative transfer

- *Steiner (1991, A&A 242, 290)* introduces multi-grid methods in radiative transfer. Examples of a two-level atom model and a two-dimensional atmosphere in radiative equilibrium;
- *Fabiani Bendicho, Trujillo Bueno, and Auer (1997, A&A 324, 161)* used the method in a multi-dimensional NLTE radiative transfer code for multi-level atoms;
- *Štěpán & Trujillo Bueno (2013, A&A 557, A143)* implement multigrid RT in PORTA, a three-dimensional multilevel radiative transfer code for modeling the intensity and polarization of spectral lines;
- *Bjørgen & Leenaarts (2017, A&A 599,A118)* use multi-grid in their Multi3D NLTE partial redistribution code.

## 4. Spectral line analysis (cont.)



Convergence behavior for MALI and multi-grid for a three-level Ca II atom (left) and a hydrogen atom (right) for a Bifrost atmosphere.

From *Bjørgen & Leenaarts (2017)*

## 5. Radiative transfer challenges parallelization

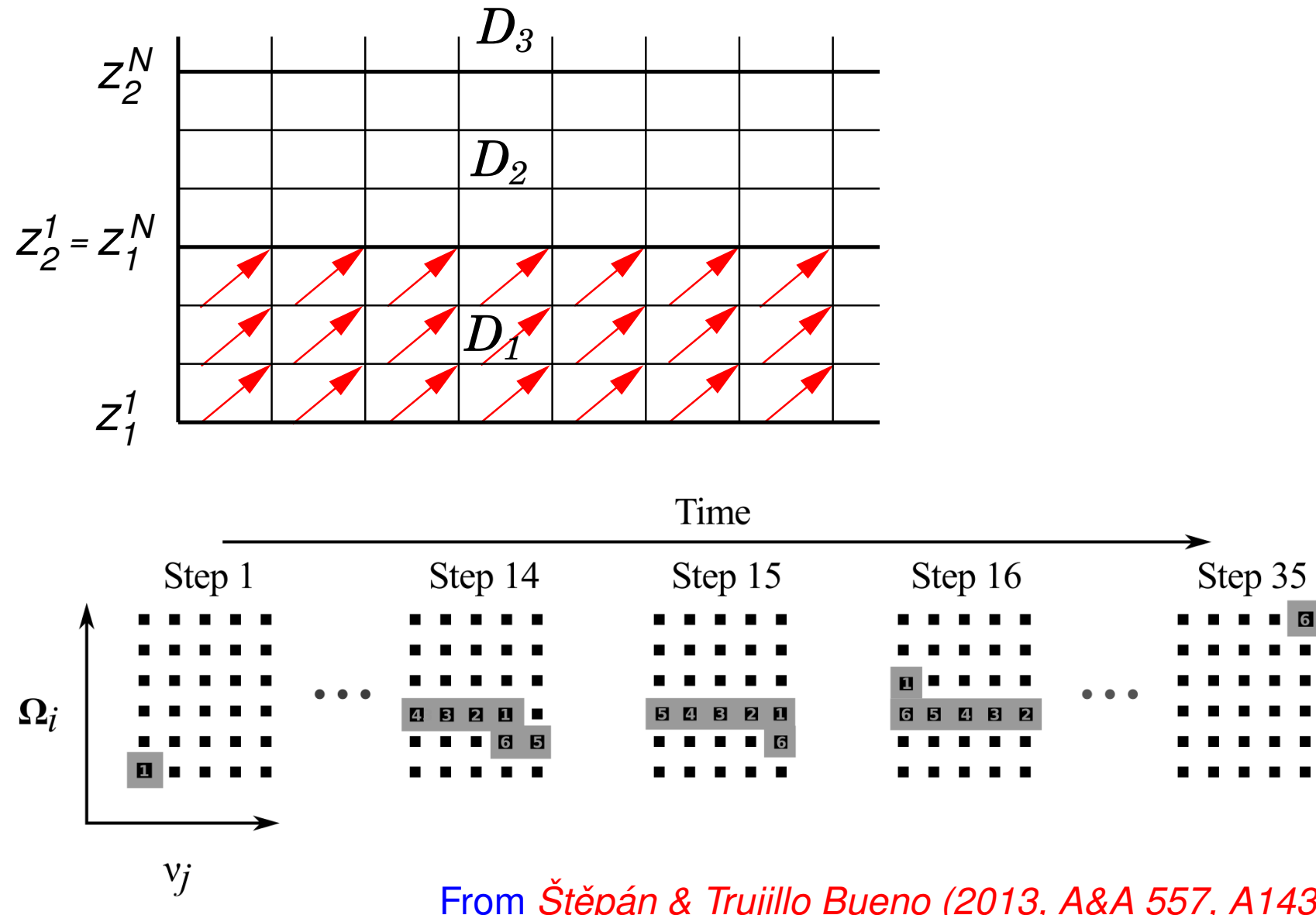
---

In time-independent radiative transfer, the mean intensity at every grid point immediately depends on the intensities at any other point in the computational domain. This renders parallelization a challenge because for the computation of the intensities in a subdomain, the boundary intensities should be known for subdomains upstream of the present one.

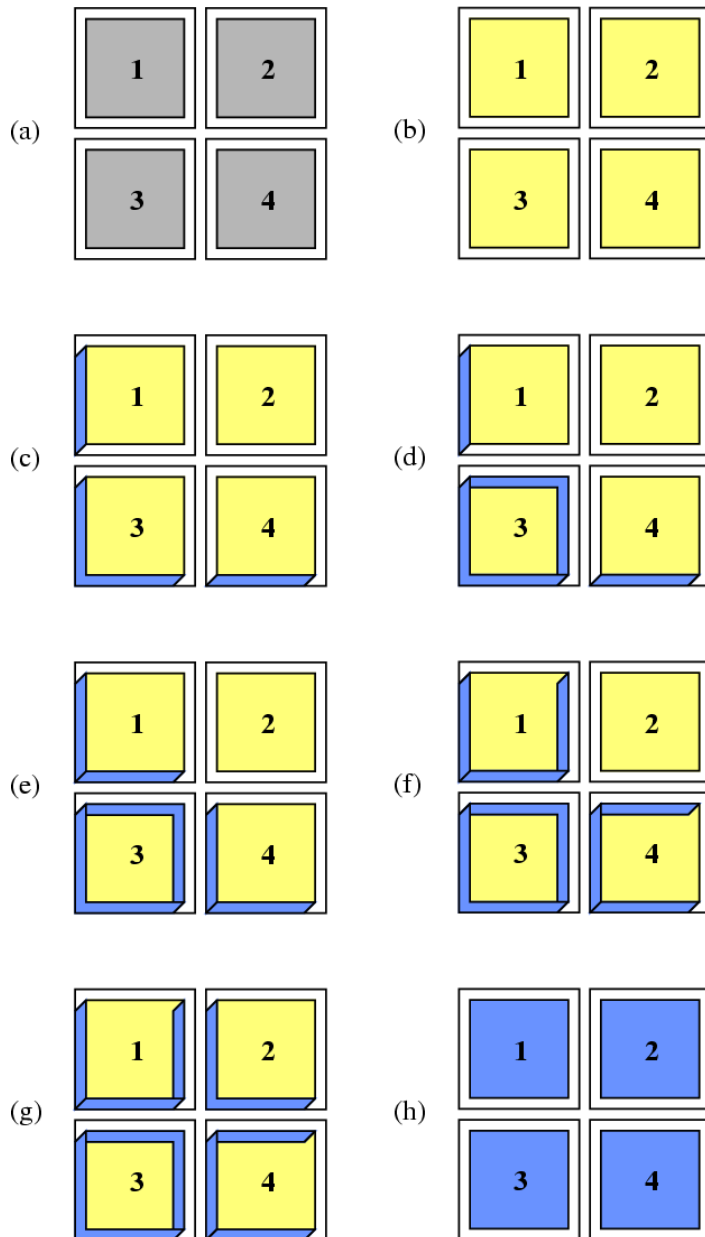
- Poor man's parallelization use for the subdomain boundaries intensities from the previous time step or iteration. (Potential troubles with radiative flux conservation.)
- If using azimuthal directions parallel to the horizontal cartesian coordinates  $x$  and  $y$  alone, domain decompositions can proceed in slabs parallel to the  $x$ - $z$ -plane and parallel to the  $y$ - $z$ -plane.
- Parallel processing of frequencies or directions.

## 5. Radiative transfer challenges parallelization (cont.)

- Plane parallel domain decomposition and the snake algorithm



## 5. Radiative transfer challenges parallelization (cont.)



$$I(\mathbf{r}, \mathbf{n}) = I_0 e^{-(\tau_0 - \tau)} + \int_{\tau}^{\tau_0} S(\tau') e^{-(\tau' - \tau)} d\tau'$$

The formal solution is divided into the intrinsic solution (yellow) and the boundary solution (blue). The calculation proceeds in three steps: (i) parallel processing of the intrinsic solution, (ii) sequential computation of the domain boundaries, (iii) parallel processing of the final solution.

From *Heinemann et al. (2006, A&A 448, 731)*.

## 6. Non-equilibrium Hydrogen ionization

---

Under the condition of the dynamic solar chromosphere the assumption of statistical equilibrium in the rate equations is not valid anymore.

In order to compute the *dynamic hydrogen ionization* in a three-dimensional environment, simplifications are needed. *E. Sollum* (1990, Master thesis Univ. Oslo) employs the *method of fixed radiative rates*. We then solve the time-dependent rate equations

$$\frac{\partial n_i}{\partial t} + \nabla \cdot (n_i \mathbf{v}) = \sum_{j \neq i}^{n_l} n_j P_{ji} - n_i \sum_{j \neq i}^{n_l} P_{ij}$$

$P_{ij} = C_{ij} + R_{ij}$ , where we assume that the radiation field in each transition, both, bound-bound and bound-free, can be described by a formal radiation temperature  $T_{\text{rad}}$ .

## 6. Non-equilibrium Hydrogen ionization (cont.)

In the method of fixed radiative rates we assume that the radiation field in each transition, both, bound-bound and bound-free, can be described by a formal radiation temperature:

$$J_\nu = \frac{2h\nu^3}{c^2} \frac{1}{e^{h\nu/kT_{\text{rad}}} - 1}$$

Thus, we obtain the *fixed radiative rates* for bound-bound transitions

$$R_{lu} = B_{lu} J_{\nu_0} = \frac{4\pi^2 e^2}{h\nu_0 m_e c} f_{lu} \frac{2h\nu_0^3}{c^2} \frac{1}{e^{h\nu_0/kT_{\text{rad}}} - 1}$$

$$R_{ul} = A_{ul} + B_{ul} J_{\nu_0} = \frac{g_l}{g_u} e^{h\nu_0/kT_{\text{rad}}} R_{lu}$$

$B_{lu}$ : Einstein coefficient for radiative excitation;  $f_{lu}$ : oscillator strength;

$A_{ul}$ ,  $B_{ul}$ : Einstein coefficient for spontaneous and stimulated deexcitation, respectively;  $g_{l,u}$ : statistical weights of the lower and upper level.

## 6. Non-equilibrium Hydrogen ionization (cont.)

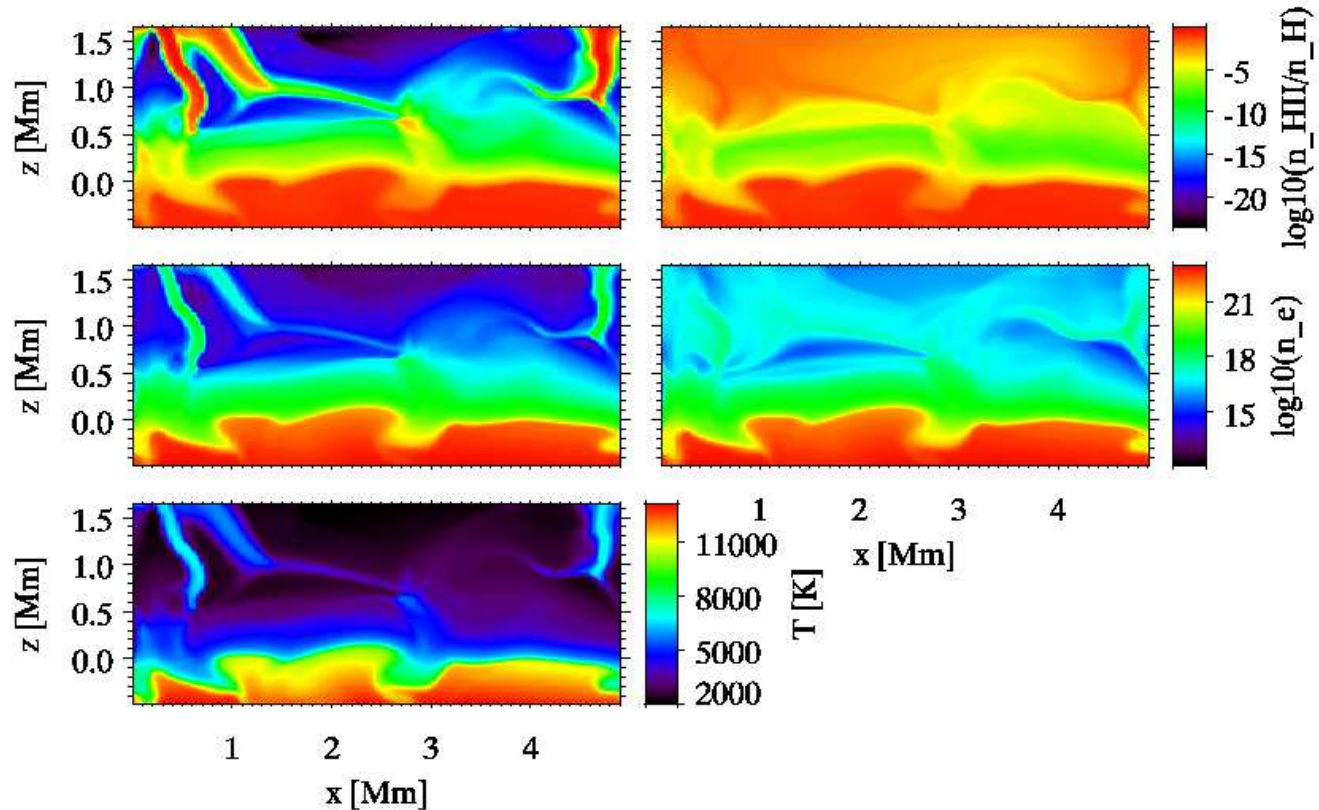
The hydrogen bound-free excitations have a Kramer's absorption cross section:

$$\sigma_{ic}(\nu) = \alpha_0 \left( \frac{\nu_0}{\nu} \right)^3, \nu > \nu_0,$$

where  $\alpha_0$  is the absorption cross-section at the edge frequency  $\nu_0$ . In this case the radiative rate coefficients are

$$\begin{aligned} R_{ic} &= 4\pi \int_{\nu_0}^{\infty} \frac{\sigma_{ic}(\nu)}{h\nu} J_{\nu} d\nu = \frac{8\pi}{c^2} \alpha_0 \nu_0^3 \int_{\nu_0}^{\infty} \frac{1}{\nu} \frac{1}{e^{h\nu/kT_{\text{rad}}} - 1} d\nu \\ &= \frac{8\pi}{c^2} \alpha_0 \nu_0^3 \sum_{n=1}^{\infty} E_1 \left[ n \frac{h\nu_0}{kT_{\text{rad}}} \right], \quad E_1 \text{ being the first exponential integral} \\ R_{ci} &= 4\pi \left[ \frac{n_i}{n_c} \right]_{\text{LTE}} \int_{\nu_0}^{\infty} \frac{\sigma_{ic}(\nu)}{h\nu} \left( \frac{2h\nu^3}{c^2} + J_{\nu} \right) e^{-h\nu/kT_e} d\nu \\ &= \frac{8\pi}{c^2} \alpha_0 \nu_0^3 \left[ \frac{n_i}{n_c} \right]_{\text{LTE}} \sum_{n=1}^{\infty} E_1 \left[ \left( n \frac{T_e}{T_{\text{rad}}} + 1 \right) \frac{h\nu_0}{kT_e} \right]. \end{aligned}$$

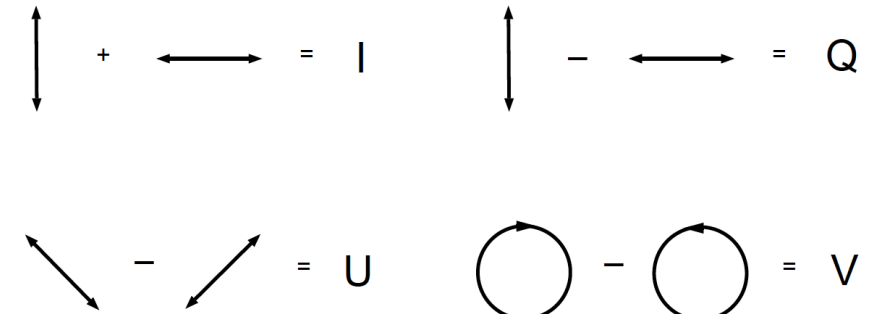
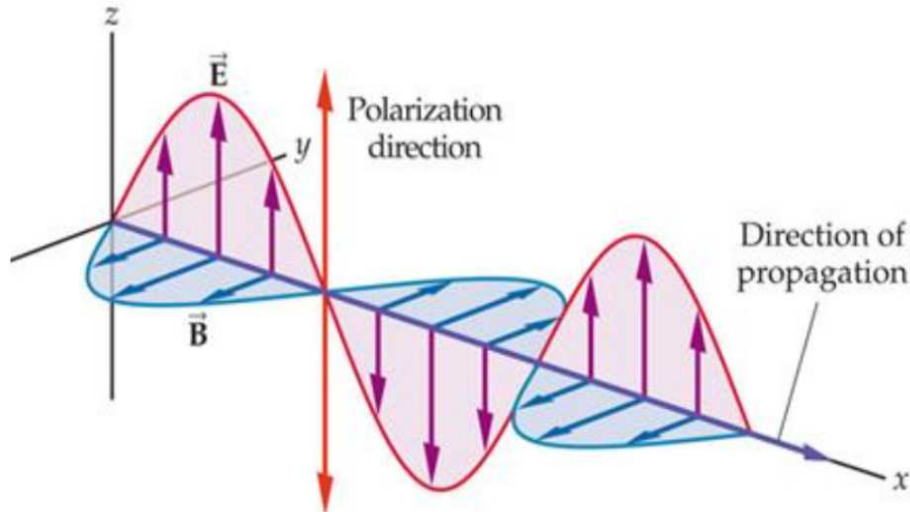
## 6. Non-equilibrium Hydrogen ionization (cont.)



Effect of dynamic H-ionization in the upper part of a 2-D simulation. *Left column: LTE* ionization degree and electron density. *Right column: Corresponding time-dependent NLTE* quantities. Bottom left: Gas temperature, which is the same for the LTE and the time-dependent case.

From *Leenaarts & Wedemeyer-Böhm 2006*.

## 7. The transfer equation for polarized light



$$\frac{d}{ds} I(s) = -\kappa(s)I(s) + \epsilon(s) \implies$$

$$\boxed{\frac{d}{ds} \mathbf{I}(s) = -\mathbf{K}(s)\mathbf{I}(s) + \boldsymbol{\epsilon}(s)}$$

$$\frac{d}{ds} \begin{pmatrix} I \\ Q \\ U \\ V \end{pmatrix} = - \begin{pmatrix} \eta_I & \eta_Q & \eta_U & \eta_V \\ \eta_Q & \eta_I & \rho_V & -\rho_U \\ \eta_U & -\rho_V & \eta_I & \rho_Q \\ \eta_V & \rho_U & -\rho_Q & \eta_I \end{pmatrix} \begin{pmatrix} I \\ Q \\ U \\ V \end{pmatrix} + \begin{pmatrix} \epsilon_I \\ \epsilon_Q \\ \epsilon_U \\ \epsilon_V \end{pmatrix}$$

## 7. The transfer equation for polarized light (cont.)

When using to the optical depth scale

$$\frac{d}{d\tau} \mathbf{I}(\tau) = \tilde{\mathbf{K}}(\tau) [\mathbf{I}(\tau) - \mathbf{S}(\tau)] ,$$

where

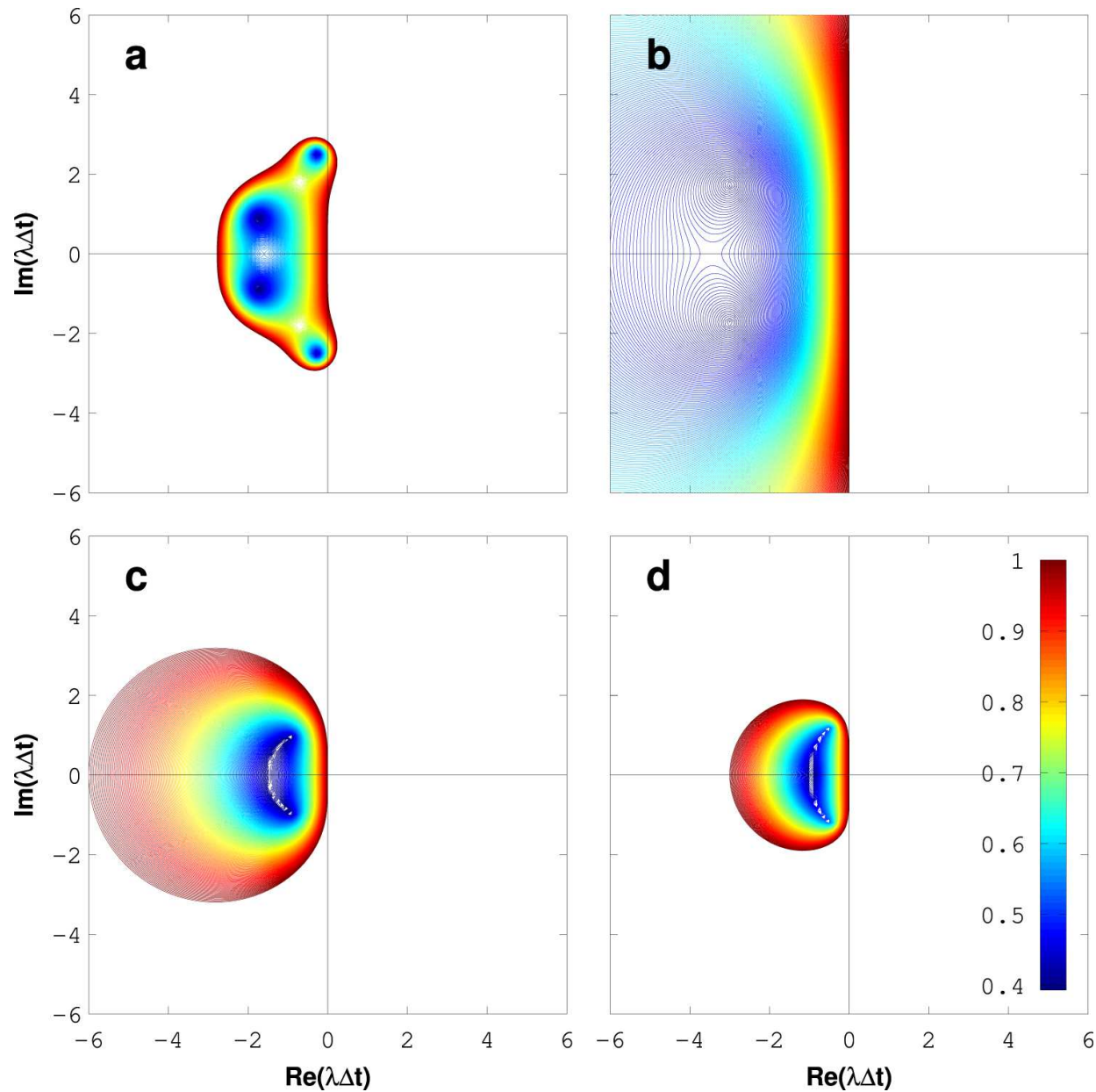
$$\tilde{\mathbf{K}} = \mathbf{K}/\eta_I = \begin{pmatrix} 1 & h_Q & h_U & h_V \\ h_Q & 1 & r_V & -r_U \\ h_U & -r_V & 1 & r_Q \\ h_V & r_U & -r_Q & 1 \end{pmatrix} \quad \text{and} \quad \mathbf{S} = \frac{\epsilon}{\eta_I}$$

The formal solution can be written in terms of the evolution operator  $\mathbf{O}$  as

$$\mathbf{I}(\tau) = \mathbf{O}(\tau, \tau') \mathbf{I}(\tau') + \int_{\tau}^{\tau'} \mathbf{O}(\tau, \tau'') \mathbf{K}(\tau'') \mathbf{S}(\tau'') d\tau'', \quad \text{with}$$

$$\mathbf{O}(\tau, \tau') = e^{-\int_{\tau}^{\tau'} \mathbf{K}(\tau'') d\tau''} = \sum_{i=1}^4 e^{-(\tau' - \tau) \lambda_i} \mathbf{N}_i \quad \text{for } \mathbf{K} = \text{const.}$$

## 7. The transfer equation for polarized light (cont.)



Stability regions for  
(a) the Runge-Kutta 4,  
(b) cubic Hermitian,  
(c) Adams- Moulton 3, and  
(d) Adams-Moulton 4  
methods. The cubic  
Hermitian method shows  
A-stability, while all other  
methods have bounded  
stability regions. From  
*Janett et al. (2017, ApJ  
845:104)*.

## 7. The transfer equation for polarized light (cont.)

A good and stable way to do this proceeds again by *operator splitting*:

$$\tilde{\mathbf{K}} = \mathbf{E} + (\tilde{\mathbf{K}} - \mathbf{E}) = \mathbf{E} + \mathcal{K}$$

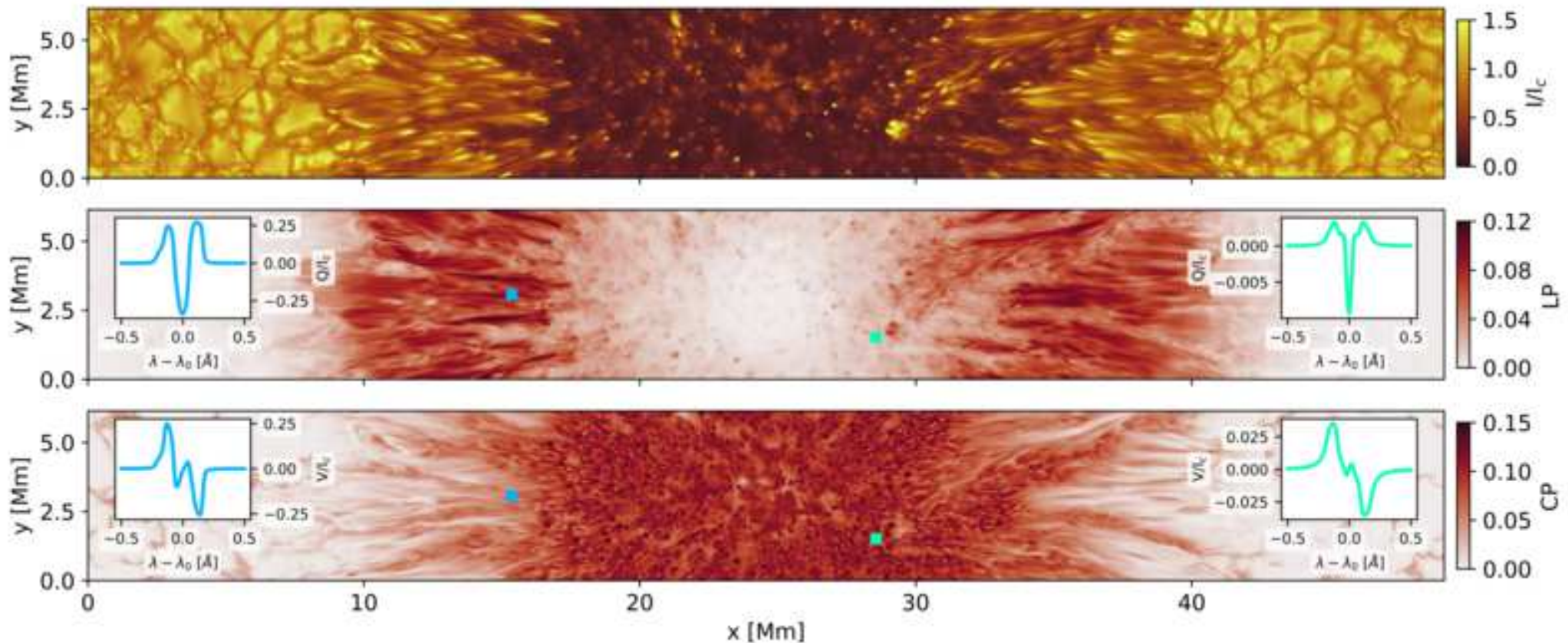
$$\begin{aligned} \frac{d}{d\tau} \mathbf{I}(\tau) &= \tilde{\mathbf{K}}(\tau) [\mathbf{I}(\tau) - \mathbf{S}(\tau)] = \mathbf{E} \mathbf{I}(\tau) + \underbrace{\mathcal{K} \mathbf{I}(\tau) - \tilde{\mathbf{K}} \mathbf{S}(\tau)}_{-\mathcal{S}(\tau, \mathbf{I})} \\ &\implies \left[ \frac{d}{d\tau} - \mathbf{E} \right] \mathbf{I}(\tau) = -\mathcal{S}(\tau, \mathbf{I}(\tau)) \end{aligned}$$

The *formal solution* is then given by

$$\mathbf{I}(\tau) = e^{(\tau - \tau_0)} \mathbf{I}_0 - \int_{\tau_0}^{\tau} e^{(\tau - \tau')} \mathcal{S}(\tau', \mathbf{I}(\tau')) d\tau',$$

where the integral is evaluated with the effective source function  $\mathcal{S}(\tau)$  approximated by a polynomial  $\mathbf{P}_q$  of degree  $q$  in the interval  $[\tau_k, \tau_{k+1}]$ . The integral can then be evaluated yielding an implicit or explicit linear system for the Stokes vector  $\mathbf{I}_{k+1}$ .

## 7. The transfer equation for polarized light (cont.)

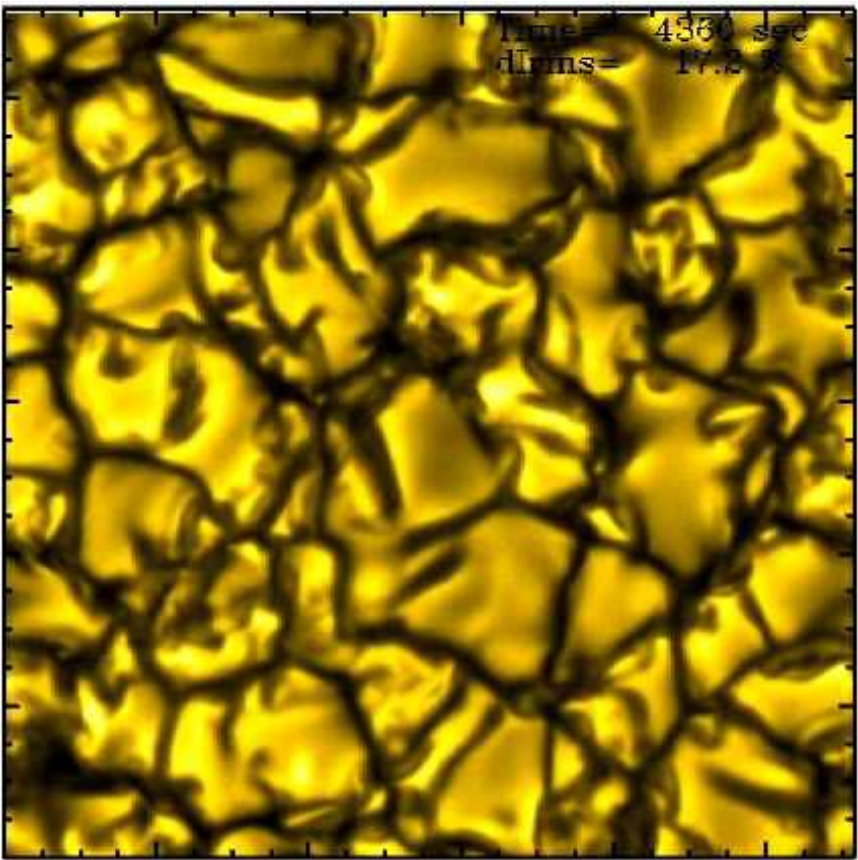


*Top panel:* Continuum intensity map; *middle panel:* linear polarization map; *bottom panel:* the circular polarization map, all of the spectral line  $Fe\text{ I }6173.344 \text{ \AA}$ . Two examples of Stokes  $Q$  and Stokes  $V$  profiles at two locations.

Courtesy, *J.-M. Borrero*.

## 8. Box in a star vs. star in a box

*Box in a star*



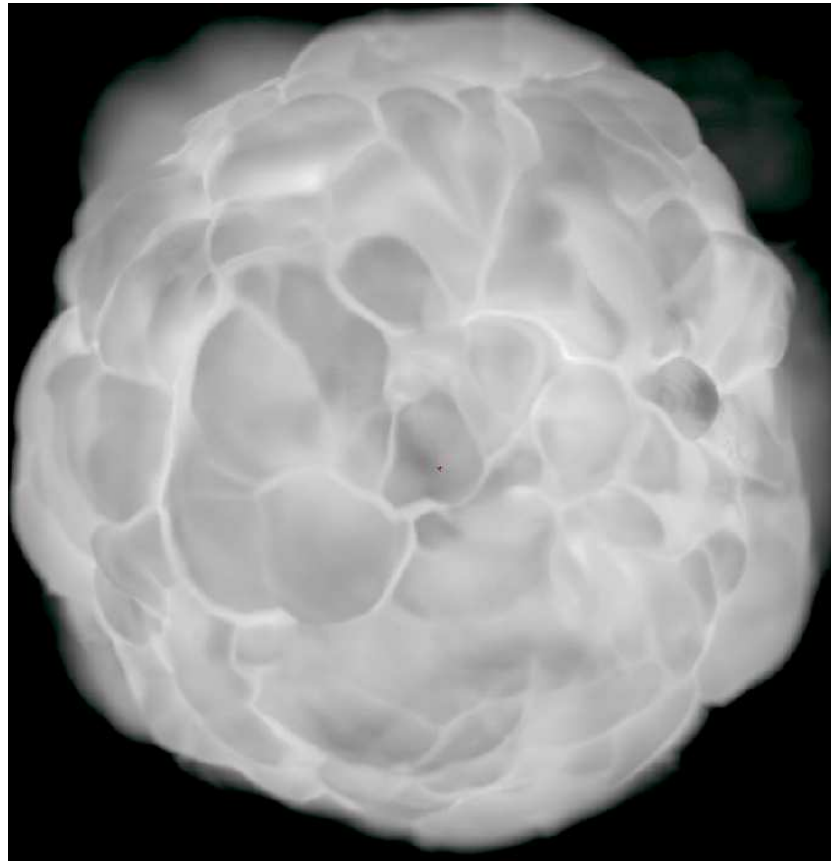
Simulation of *solar granulation with CO<sup>5</sup>BOLD*.

$400 \times 400 \times 165$  grid cells,  $11.2 \times 11.2$  Mm,

Contrast at  $\lambda \approx 620$  nm is 16.65%.

Courtesy *M. Steffen*, AIP Potsdam

*Star in a box*



Simulation of a *Betelgeuse with CO<sup>5</sup>BOLD*.

$235^3$  grid cells,  $m_{\text{star}} = 12m_{\odot}$ ,

$T_{\text{eff}} = 3436$  K,  $R_{\text{star}} = 875R_{\odot}$

Courtesy *Bernd Freytag*, Uppsala

# Table of content

---

1. Introduction
  2. Radiation transfer for stellar atmospheric simulations
  3. Multi-group radiation transfer
  4. Spectral line analysis
  5. Radiative transfer challenges parallelization
  6. Non-equilibrium Hydrogen ionization
  7. The transfer equation for polarized light
  8. Box in a star vs. star in a box
- References

## References

- Bjørgen, J.P., Leenaarts, J., Rempel, M., Cheung, M.C.M., Danilovic, S., de la Cruz Rodríguez, J., and Sukhorukov, A.V.: 2018, *Three-dimensional modeling of chromospheric spectral lines in a simulated active region*, A&A, submitted
- Bjørgen, J.P. and Leenaarts, J.: 2017, *Numerical non-LTE 3D radiative transfer using a multigrid method*, A&A 599, A118
- Calvo, F., Steiner, O., & Freytag, B.: 2016, *Non-magnetic photospheric bright points in 3D simulations of the solar atmosphere*, A&A, 596, A43
- Fabiani Bendicho, P., Trujillo Bueno, J., and Auer, L.: 1997, *Multidimensional radiative transfer with multilevel atoms. II. The non-linear multigrid method*, A&A 324, 161
- Hayek, W., Asplund, M., Carlsson, M., Trampedach, R., Collet, R., Gudiksen, B.V., Hansteen, V.H., and Leenaarts, J.: 2010, *Radiative transfer with scattering for domain-decomposed 3D MHD simulations of cool stellar atmospheres: Numerical methods and application to the quiet, non-magnetic, surface of a solar-type star*, A&A 517, A49
- Heinemann, T., Dobler, W., Nordlund, Å. and Brandenburg,A.: 2006, *Radiative transfer in decomposed domains*, A&A 448, 731
- Janett, G., Steiner, O., and Belluzzi, L.: 2017, *Formal Solutions for Polarized Radiative Transfer. II. High-order Methods*, ApJ 845, 104

Ludwig, H.-G.: 1992, *Nichtgrauer Strahlungstransport in numerischen Simulationen stellarer Konvektion*, Ph.D. thesis, Christian-Albrechts-Universität, Kiel

Leenaarts, J. and Wedemeyer-Böhm, S.: 2006, *Time-dependent hydrogen ionisation in 3D simulations of the solar chromosphere. Methods and first results*, A&A 460, 301-307

Nordlund, Å: 1982, *Numerical simulations of the solar granulation*, A&A 107, 1-10

Salhab, R.G., Steiner, O., Berdyugina, S.V., Freytag, B., Rajaguru, S.P., and Steffen, M.: 2017, *Simulation of the small-scale magnetism in main sequence stellar atmospheres*, A&A, 614, A78

Sollum, E.: 1999, Master thesis, University of Oslo, Norway

Steffen, M.: 2017, *Radiation transport in CO5BLD: A short characteristic module for local box models*, Mem. Soc. Astr. Italiana 88, 22

Steiner, O.: 1991, *Fast solution of radiative transfer problems using a method of multiple grids*, A&A 242, 290

Štěpán, J. and Trujillo Bueno, J.: 2013, *PORTA: A three-dimensional multilevel radiative transfer code for modeling the intensity and polarization of spectral lines with massively parallel computers*, A&A 557, A143